

# Effects of disc asymmetries on astrometric measurements

## Can they mimic planets?

Q. Kral<sup>1</sup>, J. Schneider<sup>2</sup>, G. Kennedy<sup>1</sup>, and D. Souami<sup>3</sup>

(1) Institute of Astronomy, University of Cambridge, Madingley Road, Cambridge CB3 0HA, UK

(2) Observatoire de Paris, LUTH-CNRS, UMR 8102, 92190, Meudon, France

(3) NaXys, University of Namur, Rempart de la Vierge 8, 5000 Namur, Belgium

e-mail: qkral@ast.cam.ac.uk, jean.schneider@obspm.fr

Received ; accepted

### ABSTRACT

Astrometry covers a parameter space that cannot be reached by RV or transit methods to detect terrestrial planets on wide orbits. In addition, high accuracy astrometric measurements are necessary to measure the inclination of the planet's orbits. Here we investigate the principles of an artefact of the astrometric approach. Namely, the displacement of the photo-centre due to inhomogeneities in a dust disc around the parent star. Indeed, theory and observations show that circumstellar discs can present strong asymmetries. We model the pseudo-astrometric signal caused by these inhomogeneities, asking whether a dust clump in a disc can mimic the astrometric signal of an Earth-like planet. We show that these inhomogeneities cannot be neglected when using astrometry to find terrestrial planets. We provide the parameter space for which these inhomogeneities can affect the astrometric signals but still not be detected by mid-IR observations. We find that a small cross section of dust corresponding to a cometary mass object is enough to mimic the astrometric signal of an Earth-like planet. Astrometric observations of protoplanetary discs to search for planets can also be affected by the presence of inhomogeneities. Some further tests are given to confirm whether an observation is a real planet astrometric signal or an impostor. Eventually, we also study the case where the cross section of dust is high enough to provide a detectable IR-excess and to have a measurable photometric displacement by actual instruments such as Gaia, IRAC or GRAVITY. We suggest a new method, which consists in using astrometry to quantify asymmetries (clumpiness) in inner debris discs that cannot be otherwise resolved.

**Key words.** astrometry: Planetary systems - discs

## 1. Introduction

The search for and observation of exoplanets is growing in three directions: new detection techniques are still emerging, ever more planets being discovered and more data being collected on each planet. The detection techniques have each their specificities regarding the accessible planet observables. Among them, astrometry is still in its infancy since, as of January 2016, only a handful of astrometric detections of exoplanet candidates have been announced, namely DE0823-49 b (Sahlmann et al. 2015) and HD 176051 b (Muterspaugh et al. 2010). Another candidate, VB 10 b, claimed to be detected by astrometry (Pravdo & Shaklan 2009), has been challenged by Bean et al. (2010) and by Anglada-Escudé et al. (2010). We shall present a plausible reason that reconciles the three studies in the discussion. This technique has yet a promising capability, which is to detect low mass planets, determine the geometry of their orbits, and more importantly measure their masses.

Just like any technique, astrometry has its own source of noise and artefacts. Until now, the only noise source limiting the sensitivity to low masses that was investigated is the activity of the central star. The latter introduces indeed a

fluctuation of the centroid of the star position (Lagrange et al. 2011).

Here we investigate an artefact of the astrometric approach, first emphasised by Schneider (2011), whose preliminary results showed that an astrometric signal subject to a perturbation by an axially asymmetric dust disc can mimic the dynamical effect of planetary companions.

This study is important in the context of astrometric projects aiming at the detection of Earth-like planets in the Habitable Zone of nearby stars (e.g. NEAT, Malbet et al. 2012). On the ground, the GRAVITY (Lacour et al. 2014) and SKA (Fomalont & Reid 2004) instruments or projects have an astrometric accuracy of a few microarcsec. For Earth-like planets, the astrometric signal expected is on the order of  $0.3 \mu\text{as}$  around a sun-like star at 10 pc (see Eq. 2) and artefacts of this order of magnitude could mimic such planets. Therefore they have to be taken into account.

We first present the general mathematical formalism in section 2 and show how it works on a range of cases in section 3. In section 4 we provide some tests to discriminate a disc-induced artefact from a real stellar wobble. Finally, we compare the effect of inhomogeneities to the performance of present and future astrometric instruments such as Gaia (de Bruijne 2012), GRAVITY, TMT (Sanders 2013) and NEAT. Furthermore, we discuss a new interesting detection technique to observe clumpiness in discs.

Send offprint requests to: Q. Kral, J. Schneider

## 2. Impact of inhomogeneities on parent star astrometry

In this section we consider the case of stellar light reflected by some dust inhomogeneities as well as its thermal emission. The point of using astrometry is to reach accuracy below the resolution of the system. In this study, we are thus interested in inhomogeneities that cannot be resolved. For this reason, the dust creating these inhomogeneities must be close to its host star. For an observation at a wavelength  $\lambda$  with a telescope of diameter  $d$ , the typical spatial resolution is  $\lambda/d$  meaning that for NEAT in the optical, the resolution is  $\sim 0.1$  arcsec. As a result, inhomogeneities that would affect astrometric measurements without being resolved will be within  $0.1''$ , i.e. within 1au (10au) for a system at 10pc (100pc).

The brightness distribution of inhomogeneities is a function of time since the disc structure evolves essentially according to its Keplerian motion. Thus, the difference in position between the star and the displacement due to the presence of an asymmetric disc can be given as a function of the inhomogeneity to star flux ratio  $I_{\text{inh}}/I_{\star}$ . If a companion is present, it also changes the observed position of the star and this is what is used to detect planets with astrometric measurements.

As astrometry is performed below the resolution limit, we observe the displacement of the photo-centre of the system. The global photo-centre displacement  $\Delta\alpha$  is a superposition of the barycentric dynamical astrometric displacement  $\Delta\alpha_B$  and the photo-centric displacement  $\Delta\alpha_{ph}$  due to the asymmetric brightness distribution of the unresolved disc (see Fig. 1).

Let  $\alpha_{ph}$  be the angular separation of the photo-centre of an inhomogeneity in the disc, of brightness ratio  $I_{\text{inh}}/I_{\star}$ , with respect to the parent star. Then the star+inhomogeneity photo-centre position has an angular offset  $\Delta\alpha_{ph}$  with respect to the parent star's centroid given by

$$\Delta\alpha_{ph} = \frac{I_{\text{inh}}}{I_{\star}} \alpha_{ph}. \quad (1)$$

By definition, neglecting the mass of the disc inhomogeneities, the barycentric displacement due to a companion with mass  $M_C$  gives

$$\Delta\alpha_B = \frac{M_C}{M_{\star}} \alpha_C, \quad (2)$$

where  $\alpha_C = a/D$  is the angular separation of the companion,  $a$  is the barycentre-planet distance projected on the sky at the measurement epoch and  $D$  the distance of the star to the observer.

Let us now assume that the photo-centre displacement is created by an inhomogeneity at distance  $a$  so that  $\alpha_{ph} = a/D$  and the amplitude of the displacement  $\Delta\alpha = I_{\text{inh}}/I_{\star}(a/D)$ , where  $a$  is in au,  $D$  in pc and  $\Delta\alpha$  in arcsec.

First, we plot on Fig. 2  $I_{\text{inh}}/I_{\star}$  as a function of  $a$  assuming a distance  $D = 10$  pc, for different values of  $\Delta\alpha$  (black solid lines). As given by Eq. 1, when  $I_{\text{inh}}/I_{\star}$  increases, for a given  $a/D$ ,  $\Delta\alpha$  increases. Also, for a given  $\Delta\alpha$ ,  $I_{\text{inh}}/I_{\star} \propto 1/a$ . The location of an Earth-like planet in terms of its  $\Delta\alpha$  needed at 1au to mimic an Earth is shown

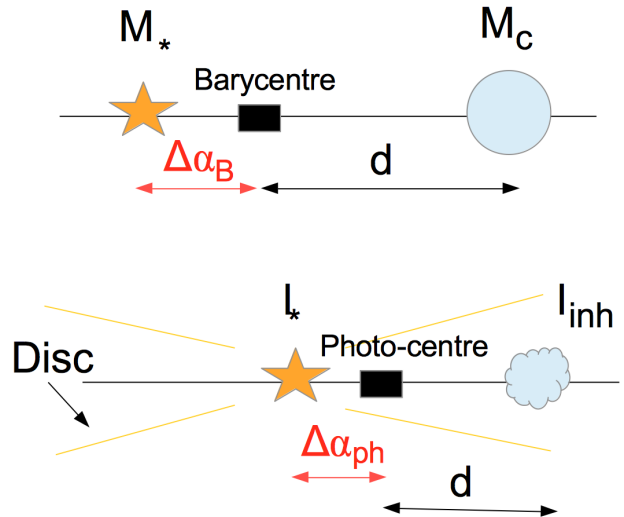


**Fig. 1.** *Top:* Schematic of the usual barycentric photo-centre displacement  $\Delta\alpha_B$  used in astrometry to detect a planet of mass  $M_C$  at distance  $a$  from the barycentre with the star of mass  $M_{\star}$ . *Bottom:* The photo-centre displacement  $\Delta\alpha_{ph}$  is now caused by an inhomogeneity of flux  $I_{\text{inh}}$  at distance  $a$  orbiting around a star of flux  $I_{\star}$  and possibly surrounded by a disc shown with yellow lines.

as a red square in Fig. 2. This gives the inhomogeneity-to-star flux ratio required to mimic an Earth. On the right plot, this location changes as the host star is more massive by a factor  $\sim 1.8$ . Indeed, using Eq. 2, we can rewrite it in these more useful terms:

$$\Delta\alpha_B = 0.3\mu\text{as} \frac{M_p}{M_{\oplus}} \left(\frac{M_{\star}}{M_{\odot}}\right)^{-1} \frac{a'}{1\text{au}} \left(\frac{D}{10\text{pc}}\right)^{-1}. \quad (3)$$

Simply assuming that habitable planets around more or less luminous stars reside at distances where the insolation is equal to the Earth's, then  $a' = a(L_{\star}/L_{\odot})^{0.5}$  is the new location of the planet. The location of an Earth-like planet around  $\beta$  Pic is then at  $a' = 2.83$  au and would imply a displacement of  $0.47\mu\text{as}$ .

We assess the detectability of such inhomogeneities using the WISE detection limits at  $\lambda_{\text{lim}}=12\mu\text{m}$ . At a given astrometric observing wavelength  $\lambda_{\text{inh}}$  we compute the minimum value of  $I_{\text{inh}}/I_{\star}$  that could be detected by WISE at different  $a$ . To do so, we assume that the detections are limited by our ability to differentiate the WISE photometry from the stellar flux (“calibration limited”) and that the grains behave like pseudo-black bodies with an albedo  $\omega = 0.2$ . We find that in thermal emission, the minimum detected flux ratio at wavelength  $\lambda_{\text{inh}}$  is given by

$$\frac{I_{\text{inh}}}{I_{\star}}(\lambda_{\text{inh}}) = R_{\text{lim}} \frac{B_{\nu}(\lambda_{\text{inh}}, T)}{B_{\nu}(\lambda_{\text{inh}}, T_{\star})} \frac{B_{\nu}(\lambda_{\text{lim}}, T_{\star})}{B_{\nu}(\lambda_{\text{lim}}, T)}, \quad (4)$$

where  $B_{\nu}$  is the Planck function and  $R_{\text{lim}}$  is the WISE calibration limit ( $\sim 10\%$ ). To get this formula, we compute the disc-to-star flux ratio at a certain wavelength  $\lambda_{\text{lim}}$  set by the WISE sensitivity and shift it to another (thermal) wavelength  $\lambda_{\text{inh}}$  where the astrometry is done. The albedo does not appear in this equation as it affects both the WISE

and the astrometric wavelengths equally. Similarly, in scattered light, converting the thermal detection limit to an optical flux, this limit is defined by

$$\frac{I_{\text{inh}}}{I_{\star}}(\lambda_{\text{inh}}) = 6 \times 10^9 \frac{\omega}{1 - \omega} \frac{R_{\text{lim}}}{a^2} \frac{B_{\nu}(\lambda_{\text{lim}}, T_{\star})}{B_{\nu}(\lambda_{\text{lim}}, T)} \frac{L_{\star}}{T_{\star}^4}, \quad (5)$$

where  $L_{\star}$  is the star’s luminosity in solar luminosity,  $T_{\star}$  the star’s temperature (in K), and  $a$  is in au.  $T = 278.3 L_{\star}^{0.25} / \sqrt{a}$  is the black body temperature of the inhomogeneity. We assumed that the absorption/scattering properties are wavelength independent (i.e. albedo is monochromatic) but we illustrate what happens in Fig. 3 for a full Mie calculation.

The red curves on Fig. 2 show the corresponding limits for different observing wavelengths  $\lambda_{\text{inh}}$  equal to 0.55 (solid line, for Gaia, NEAT), 2.2 (dotted line, for GRAVITY) and 20 (dashed line, for TMT)  $\mu\text{m}$ . The left plot is for the case of a sun-like star and the right plot for a  $\beta$  Pic-like star. In this last case, we consider an Earth-like planet as having the same irradiation and mass as Earth, so it is located at 2.83au as stated earlier when defining  $a'$ . Above each red line, the dust inhomogeneity could be detected by WISE at  $12\mu\text{m}$ . One can notice the wide range of the parameter space where some dust could be undetected but still create a photo-centre displacement big enough to mimic an Earth-like planet. The limits on the amount of dust depend on the type of host star (which changes the dust temperature) as well as  $\lambda_{\text{inh}}$ . For observations of the astrometric displacement in the optical, the emission is dominated by scattered light whilst at  $20\mu\text{m}$ , only thermal emission is present. For the  $\lambda_{\text{inh}} = 2.2$  microns case shown on the plot, both thermal emission and scattered light can be important depending on the distance to the star, which explains the two regimes observed on the dotted line. Indeed, for a sun-like ( $\beta$  Pic like) star, within 0.2au (0.8au), the grains are so hot that thermal emission becomes dominant over scattered light. We conclude here that there is still a large parameter space (which gets larger for lower mass stars) where inhomogeneities can be bright enough to induce a photo-centre displacement but still be undetectable. Of course, the detection of an IR-excess in a system with an astrometric detection does not guarantee that the dust is the cause, as the dust distribution could be axisymmetric.

### 3. Various cases of inhomogeneities in planetary systems

#### 3.1. Overview of the different cases

The inhomogeneities presented in the previous section can be classified in two different categories of axial asymmetries in discs: static and non static. Beyond that general dichotomy, it is not trivial to describe the diversity of asymmetric morphologies by a limited number of categories. One could imagine diverse situations such as “bright spots”, “vortices”, “spiral structures” or even “giant impacts”. The static inhomogeneities lead to a photo-centre displacement that is constant in time and can therefore not mimic the stellar motion due to a companion. Thus, the only inhomogeneities that we are interested in are non static configurations. For this reason, we discard giant impacts, which show a strong asymmetry at the collision point at steady state but that does not move and could be distinguished from a planet

(Kral et al. 2015). For the same reasons, the warps in discs (created by an inclined planet) and pericentre glow effects (brightness asymmetry due to secular perturbations by an eccentric planet, leading to an eccentric disc) are discarded. The interesting cases that could affect astrometric measurements can be summed up as follow:

- 1) Bright spots (dust cloud in a disc, clumps due to a resonance with a planet),
- 2) Spiral structures (due to a planetary companion or a fly-by with a nearby star),
- 3) Inhomogeneities in protoplanetary discs (vortices, planet induced spirals, ...)
- 4) Non static others

Let us now parametrise the different non static configurations listed above relaxing the previous black body assumption and assess their respective impacts on astrometric observations.

- “Bright spots”

Bright spots are observed in discs and are expected from theory. These bright spots could be dust clouds that are created by dust produced in collisions between planetesimals within an otherwise undetectable debris disc (Wyatt & Dent 2002; Zeegers et al. 2014). One could also imagine that the spots are dust clumps that stay within the Hill sphere of planetesimals. These enshrouded planetesimals are surrounded by a swarm of irregular satellites that collide and create the dust cloud (Kennedy & Wyatt 2011). Another possibility would be that planetesimals are surrounded by rings such as the centaur Chariklo (Braga-Ribas et al. 2014), but more massive and with a high albedo. These clumps are also expected trailing behind planets, as in the Earth’s resonant ring that corotates with Earth (Wyatt et al. 1999). More generally, dust grains can be trapped in mean-motion resonances with planets when migrating inwards due to Poynting-Robertson drag, which can create luminous dust clumps (e.g. Shannon et al. 2015). We do not intend to be exhaustive here but rather give an idea of several configurations that could create these bright spots.

In this case, we can use Eq. 1, where  $I_{\text{inh}} = I_{\text{spot}}(a_s, \lambda)$ , the spot flux at wavelength  $\lambda$  and at a projected distance  $a_s$  that we shall assume to be the semi-major axis of the dust cloud for simplicity. Also,  $\alpha_{\text{ph}} = a_s/D$ , where  $D$  is the distance to Earth.  $I_{\text{spot}}$  is the sum of thermal emission  $I_{\text{spot}_{\text{th}}}$  and scattered light  $I_{\text{spot}_{\text{sca}}}$ .  $I_{\text{spot}_{\text{th}}}$  (assuming a fixed composition) is equal to

$$I_{\text{spot}_{\text{th}}} = \int_{s_{\text{min}}}^{s_{\text{max}}} \frac{\sigma_{\text{abs}}(\lambda, s)}{4D^2} B_{\nu}(T_s(a_s, s)) dN(s), \quad (6)$$

where  $\sigma_{\text{abs}}$  is the absorption/emission cross section of the cloud for a given grain size  $s$ , i.e.  $4\pi s^2 Q_{\text{abs}}(s, \lambda)$  and  $B_{\nu}(T_s)$  is the Planck function for a temperature  $T_s$ .  $Q_{\text{abs}}$  is the dimensionless absorption/emission coefficient, which for a given grain size depends only on the wavelength  $\lambda$ .  $dN(s) \propto s^{-q} ds$  is the size distribution of grains. We choose the standard  $q = 3.5$  value to model dust clouds (e.g. Kral et al. 2013). The grain temperature  $T_s$  is worked out solving the thermal equilibrium of grains using the code GRaTeR (Augereau et al. 1999;

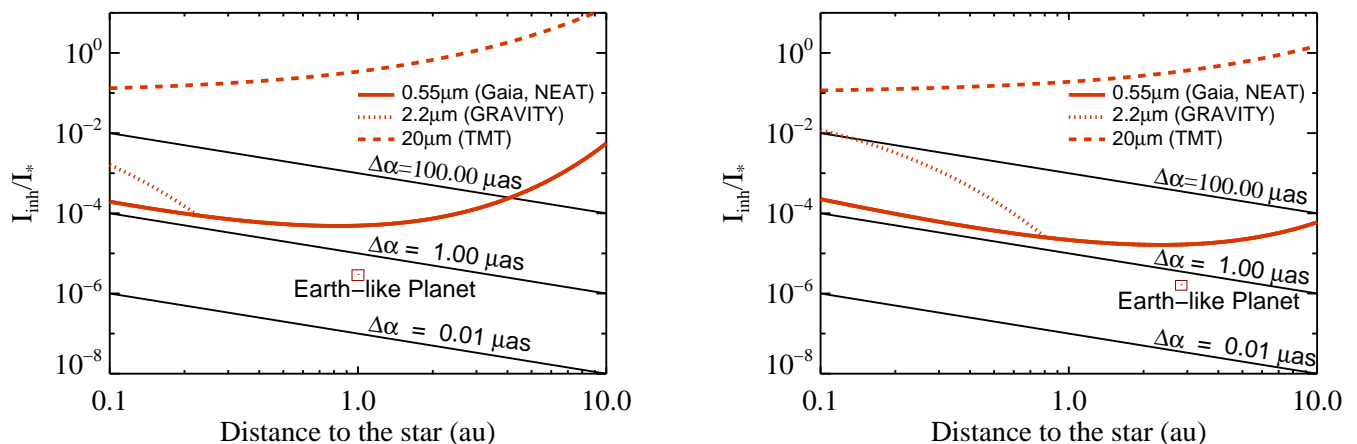


**Fig. 2.** *Left:*  $I_{\text{inh}}/I_*$  as a function of the distance to the star  $a$  (in au) for different photo-centre displacements ( $\Delta\alpha = [0.01, 1, 100]$   $\mu\text{as}$ ) in black solid lines. WISE ( $12\mu\text{m}$ ) detection limit in terms of  $I_{\text{inh}}/I_*$  are shown in red for a dust cloud orbiting at  $a$  around a sun-like star and observed at different wavelengths representing different potential instruments, 0.55 (solid, Gaia or NEAT), 2.2 (dotted, GRAVITY) and 20 ( $\mu\text{m}$ , TMT) microns. The position of an Earth-like planet is represented with a red square. *Right:* Same for a dust cloud orbiting a  $\beta$ -Pic like A6V star. In this case, the Earth-like planet having the same irradiation and mass as Earth is located at 2.83au (see text for details).

Lebreton et al. 2013). Indeed, for small grains the black body assumption is far from being accurate and as we are interested in the whole wavelength range for astrometric measurements, we assess the infrared emission from the dust properly through Eq. 6. Similarly, for the case of scattered light

$$I_{\text{spot}_{\text{sca}}}(a_s, \lambda) = I_*(\lambda) f(\phi) \frac{\sigma_{\text{sca}}(\lambda)}{a_s^2}, \quad (7)$$

where  $\sigma_{\text{sca}}(\lambda) = \int_{s_{\text{min}}}^{s_{\text{max}}} \pi s^2 Q_{\text{sca}}(s, \lambda) dN(s)$ ,  $Q_{\text{sca}}$  being the dimensionless scattering coefficient and  $f(\phi)$  is the phase function, which is equal to  $1/4\pi$  as we assume isotropic scattering.

#### – “Spiral structures”

Two types of spiral structures can develop in debris discs. Spirals due to tidal forces following the passage of, for instance, an unbound companion or over longer timescales due to differential precession for the case of a bound companion. The tidally induced spiral evolves quickly as its evolution is set up by the differential rotation of the disc  $d\Omega/dR$ , where  $\Omega$  is the orbital frequency and  $R$  the distance of planetesimals. The probability to witness such spirals is thus rather low and we do not intend to model them. For the other type of spiral, the evolution is set by the differential precession of the orbits  $d\omega_p/dR$ , where  $\omega_p$  is the precession velocity of the orbits. One finds that for a circular perturber of mass  $M_p$  and semi-major axis  $a_p$  (Augereau & Papaloizou 2004)

$$\omega_p = \frac{3GM_p}{4\Omega a_p^3}. \quad (8)$$

The evolution of this type of spirals is then very slow compared to the Keplerian evolution and could not be misinterpreted as being a planet.

#### – “Inhomogeneties in protoplanetary discs”

We created a general category for these young systems still surrounded by a protoplanetary disc and we give some specific cases that could interfere with astrometric measurements.

Vortices are expected to be present in protoplanetary discs being induced either by the Rossby-wave instabilities (RWI, Lovelace et al. 1999) or baroclinic instabilities (Lesur & Papaloizou 2010). In the case of the RWI, it can be triggered either on the edge of a gap carved by giant planets or at the interface with dead zones. These vortices can even be created very close to the star at the inner disc edge at the boundaries between turbulent, magnetised and accreting regions (Faure et al. 2015; Ansdell et al. 2016). These vortices can survive for several orbits which can be shortened depending on several complicated effects such as, for instance, the amount of turbulence or dust feedback effects (Fu et al. 2014). One such vortex was plausibly observed by ALMA (Van der Marel et al. 2013). These vortices can be, as a first approximation, modelled as we have done for dust clouds. As large dust concentrates in the vortex centre, we shall take a shallower size distribution within the affected size range as explained in Lyra & Lin (2013).

Planet induced spirals (Tanaka et al. 2002) are expected in protoplanetary discs and one could end up having both the contribution of the planet and the spirals in the astrometric measurements. Gravitational instabilities may develop in protoplanetary discs and lead to fragmentation and clump formation (e.g. Meru 2015). SAO 206462 is an example of young disc presenting spiral features that could be generated with either a planet or gravitational instability (Garufi et al. 2013). Spiral waves may also be triggered by shadows in transition discs (Montesinos et al. 2016) or even by an inflow coming from the residual external envelope of protoplanetary discs (Lesur et al. 2015).

We also note that mid-IR variability has been observed in many protoplanetary discs (Flaherty et al. 2014). This may be due to variations in the structure of the inner rim of the protoplanetary disc. Depending on the disc orientation, this would also cause an astrometric effect. The astrometric displacement derived from such a variation would also depend on the inclination, and might not look like an ellipse however, since the bright spot (the puffed up bit of rim) would not necessarily be visible for the whole orbit.

– “Others”

This subsection includes the case of many different substructures that can be found in planetary systems that shall be treated on a case by case basis. For example, the case of AU Mic shows that we do not yet fully understand all types of inhomogeneities (Boccaletti et al. 2015). In this system, some dust clumps are observed to move radially outwards with time. It can be modelled as a dust clump that is composed of unbound grains and move radially outwards.

### 3.2. Quantify the effect of inhomogeneities for some specific cases of debris and protoplanetary discs

We now evaluate the quantitative effect of disc asymmetries listed in subsection 3.1. Since we have in mind astrometric programs with timescales less than 10 years, we must consider the inner part of discs closer than 1 arcsec of the parent star. Such regions have not yet been investigated, with the exception of a few interferometric observations (e.g. Fomalhaut, Lebreton et al. 2013) and photometric light curves (Rodriguez et al. 2015). We are thus constrained to rely on models extrapolating below 1 arcsec (assuming systems close to the Earth) observations made further than 1 arcsec of the parent star.

– “Bright spots”

For this example, we shall model a dust cloud orbiting at 1au around a sun-like star at 10pc. We would like to check that Fig. 2 still holds when relaxing the black body assumption. A signal to be mistaken with an Earth-like planet, with the same orbital period and the same astrometric amplitude would create a  $0.3\mu\text{as}$  astrometric signal. It converts in  $I_{\text{inh}}/I_{\star} = 3 \times 10^{-6}$  or a total cross section  $\sigma_{\text{tot}} \sim 10^{18} \text{ m}^2$ . Thus, we input a dust cloud with a cross section of  $10^{18} \text{ m}^2$ . The minimum grain size in the dust cloud is set by radiation pressure cut-off, which is  $\sim 1$  micron for this type of host star. We fix the maximum size as being 100m, but one should note that the biggest bodies will not contribute to the flux at all. This fixes the total mass to be  $3 \times 10^{19} \text{ kg}$  (30 times lighter than Ceres). We use a conventional size distribution with  $q = 3.5$ . The photometric displacement due to the dust cloud depends on the wavelength as shown in Fig. 3. It does create a  $\Delta\alpha = 0.4\mu\text{as}$  in the optical, which is close to the expected  $0.3\mu\text{as}$  in the optical. For longer wavelength, the astrometric displacement is even larger. We overplot the results of our analytical model for varying spectral types (A6V, G2V and M8V) in Fig. 3. The values predicted

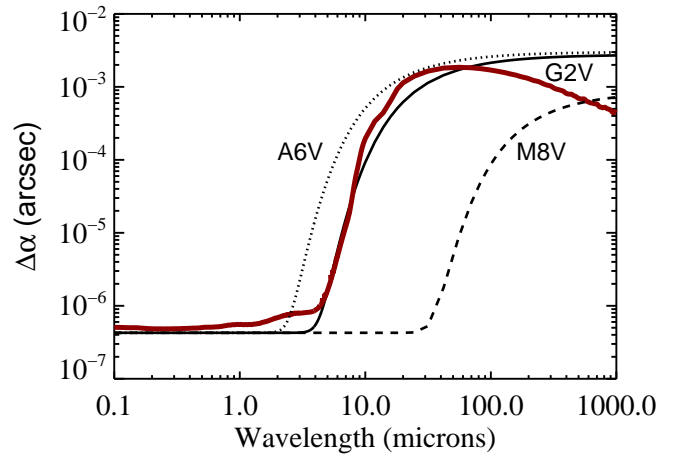


**Fig. 3.** Photo-centre displacement as a function of wavelength for a Keplerian dust cloud orbiting at 1au around a G2V star at 10pc (solid lines). The thicker of the G2V lines is the numerical model. We also vary the spectral type of the host star using the analytical model, the dotted line is for an A6V star and the dashed line for an M8V star.

with our black body assumption provide a very good estimate of the real displacement. We note two major differences. First, by comparing the numerical model (thick line) and the analytical black body assumption, one notices that they behave differently at longer wavelengths because grains are inefficient emitters when  $\lambda > s$ . Secondly, the break between the scattered light dominated regime (smaller  $\lambda$ ) and the thermal emission dominated regime happens at longer  $\lambda$  for latter spectral types (see subsection 4.3 for more details).

This implies that an undetectable cometary mass body, if broken up and distributed as a collisional cascade size distribution, is enough to create a signal greater than  $0.3 \mu\text{as}$  (which is the astrometric displacement due to an Earth-like planet at 1au at 10pc) in the optical. This dust cloud is then able to mimic an Earth-like planet as would be any more massive dust clouds. The mass is too small to change the barycentre position significantly so that the only contribution to the photo-centre displacement is from the dust cloud brightness.

– “Inhomogeneities in protoplanetary discs”

Most of the inhomogeneities presented in subsection 3.1 for protoplanetary discs could be modelled with a bright spot. For instance, vortices could easily be modelled with a dust cloud with two different size distributions as the biggest grains, with a Stokes number close to one, are most easily trapped. We emphasise however that these features are surrounded by a protoplanetary discs that should definitely be detected if present (e.g. by IR-excess). Anyway, all the cases presented in subsection 3.1 might arise, but since most of them can be modelled with a bright spot, a more refined study is left for the future when astrometric data of systems hosting a protoplanetary discs will be available.

We use Fig. 2 (right) to see that one needs  $I_{\text{inh}}/I_{\star}$  to be  $\sim 1.5 \times 10^{-6}$  to mimic an Earth-like planet around an A6V star ( $a' = 2.83\text{au}$ ) at 10pc, which translates as a total cross section equal to  $2 \times 10^{18} \text{ m}^2$ . Using this

cross section, we check with GRaTeR that the results are very similar to those presented on Fig. 3. Such a cross section is sufficient to imply a displacement of the photo-centre large enough to perturb the detection of an Earth-like planet. This confirms once again that our black body approximation on Fig. 2 gives sensible results. Indeed, the photo-centre displacement created by the inhomogeneity emission is equal to the expected  $0.45\mu\text{as}$  (see Eq. 3) in the optical and is greater at longer wavelength as is found for the bright spot case (see Fig. 3). The displacement induced at longer wavelengths could be detected by high accuracy astrometric instruments such as SKA or even using IRAC/Spitzer that can reach an astrometric precision of  $\sim 20\text{mas}$  (Esplin & Luhman 2016). This shows that astrometric observations of systems hosting protoplanetary discs may be affected by these asymmetric structures. Disentangling a real planet from these inhomogeneities requires extra work as explained in details in section 4.

– “Others”

As an example of “other” configurations we take the disc around AU Mic. It shows fast, apparently non Keplerian, motions of spots. Assuming a contrast ratio of  $10^{-5}$  relative to the parent star corresponding to the high contrast imaging performances of the images of AU Mic with SPHERE (see Boccaletti et al. 2015), the features A, B, C, D and E lead respectively to the following pseudo astrometric effects in  $\mu\text{as}$  (derived from their Figure 3b) at epochs 2011 (HST) and 2014 (SPHERE):

Image	$\alpha_{ph}$ 2011	$\alpha_{ph}$ 2014	$\Delta\alpha_{ph}$ 2014-2011
A	8	10	2
B	35	42	7
C	60	68	8
D	72	76	4
E	90	96	6

Assuming an astrometric instrument with a 1 arcsec resolution, only the spine A would have an astrometric effect on the parent star. It would lead an astrometric difference between 2011 and 2014 of  $2\mu\text{as}$ . It corresponds to an astrometric effect linear in time between 2011 to 2014; it can therefore not mimic the Keplerian motion of a companion with a period of only a few years, since the transverse velocity of the latter would be sinusoidal on an edge-on orbit.

#### 4. Tests to confirm an astrometric planet detection

Here we discuss some observational tests to check if an apparent photo-centre displacement is due to a barycentric effect by a companion or to a disc asymmetry.

##### 4.1. Comparison with radial velocity measurements

Some bright non static asymmetries could mimic a pseudo-planet sufficiently massive to be detectable by radial velocity measurements. A first trivial check would therefore consist in a monitoring of the radial velocity of the parent star, if permitted by the stellar spectrum.

The proposed test has been applied by Anglada-Escudé et al. (2010) and by Bean et al. (2010) to the planet

candidate claimed by Pravdo & Shaklan (2009) to be detected by astrometry. These authors did not detect it by radial velocity, concluding that VB 10 b does not exist. We suggest that a possible explanation of the contradiction between the astrometric claim by Pravdo & Shaklan and the negative result from radial velocities measurement consists in an astrometric effect due to an asymmetric disc inhomogeneity. We recomputed Fig. 2 for this case, where the host star has very low luminosity (M8V star) and temperature ( $\sim 2700$  K). The detection limit given by WISE for this case is very high, which would allow a massive dust cloud creating a  $\Delta\alpha_{ph}$  greater than  $1\text{mas}$  to be present without being detectable.

##### 4.2. Time evolution

If the photo-centre evolution is a stellar wobble due to a companion, it must correspond to a Keplerian motion. Such Keplerian motions are also the case for bright spots and vortices, while the cases of AU Mic or spiral evolution show that for some cases the effective photo-centre displacement may be non-Keplerian. A first test is thus to check if the displacement is Keplerian. If it is not, the wobble is not due to a companion.

Nevertheless, it is not as straightforward if there are more than one planetary companion with different periods, since the stellar wobble is then different from a simple Keplerian motion. Vice versa, if the displacement is Keplerian, it is not a proof that it is a dynamical stellar wobble as explained in this paper. The eccentricity of the object creating the astrometric signal may give some clues as for the favoured scenario: planet versus dust. Indeed, one may expect dust clouds to have a rather low eccentricity but planets can reach higher values. This could not be claimed as a secured test but give some hints to disentangle the different possibilities.

##### 4.3. Chromaticity

The dynamical stellar wobble induced by one (or more) companion is wavelength independent. In particular it must be the same in reflected light (in the visible and near-infrared domain) and in thermal regime (mid-infrared to mm). An achromaticity<sup>1</sup> of the photo-centre displacement is a strong test of its purely dynamical origin. On the contrary, an inhomogeneity would create a chromatic signal (e.g. see Fig. 3). Therefore, whenever possible, a candidate astrometric displacement should be observed in at least two wavelength regimes where a change is expected. The two observing wavelength must be chosen accordingly to the spectral type of the host star as the break between a reflected light dominated regime and a thermal emission regime happens at longer wavelength for latter spectral types (see Fig. 3). For M dwarfs, one should look in the far-IR to mm to see a difference, whereas for an early A type star, NIR or mid-IR observations will already show a difference. In any case, observing at longer wavelengths seems more favourable and SKA should be a

<sup>1</sup> We here define a chromatic signal as being wavelength dependent and an achromatic signal as being constant with varying wavelength

good instrument to realise these observations.

In the above subsection looking at comparisons with radial velocity measurements we have suggested that the pseudo astrometric detection of VB 10 b is due to an asymmetric disc inhomogeneity. A confirmation of this explanation would be that the detection of the astrometric effect detected by Pravdo & Shaklan at 550-750 nm is wavelength dependent, for instance, in the far-IR or submillimetric regimes. We recommend to observe it with, SKA, when built using astrometry or the Large Binocular Telescope Interferometer (LBTI, Defrère et al. 2016) to look for warm dust.

#### 4.4. Direct imaging

Direct imaging can be used a posteriori for a confirmation or rejection of the candidate astrometric signal. Indeed, a very strong test would consist in a high angular resolution image of the stellar environment to investigate possible non static asymmetries in a disc. Also, this is a good way to disentangle an astrometric signal coming from both an inhomogeneity and a planet (the achromaticity VS chromaticity of the signal could also be used), as would be created by an equivalent to the Earth's resonant ring that corotates with Earth (Wyatt et al. 1999). In the visible and near-infrared the GPI camera on the Magellan telescope and the SPHERE camera on the VLT and in the millimetric regime the ALMA instruments are well adapted to this task. However, direct imaging of discs is only possible for the brightest systems with a fractional luminosity greater than about  $10^{-4}$  and there are not yet any cases where a disc has been imaged but no IR-excess was detected. As for protoplanetary discs, seeing structures within a few au is not yet possible for the distances they reside at. Therefore, direct imaging could only be useful to detect the supposed planet otherwise detected by astrometry.

## 5. Discussion

Note that a byproduct of our discussion of the wavelength dependence of a pseudo-astrometric effect is to suggest to detect astrometrically inner discs not detectable by imaging and to constrain their asymmetry. It could in particular first be applied to some systems where Falling Evaporating Bodies (FEBs) are known like  $\beta$  Pictoris or HD172555 (Beust et al. 1998; Kiefer et al. 2014). It could also be tried on systems where interferometric observations seem to show the presence of hot dust called exozodis (Absil et al. 2013; Ertel et al. 2015). The final aim would be to apply this astrometric method to randomly probe the inner parts of planetary systems and discover some hidden components such as FEBs, asymmetric exozodis or even trailing clumps behind planets such as the Earth's resonant ring that corotates with Earth (Wyatt et al. 1999).

Hence, while we have shown that unseen dust in the inner regions of planetary systems may masquerade as planets, the same technique could be used to probe the structure of known warm dust populations. For example, the  $\sim 1$ Gyr old star  $\eta$  Corvi hosts both warm and cool dust components (Wyatt et al. 2005), with the warm component residing at about 1au (Smith et al. 2009; Defrère et al. 2015). The origin of the warm component is unknown, but suggested to

be the outcome of a system-wide recent or ongoing dynamical instability (Lisse et al. 2011). Recent observations with the LBTI constrained this dust to lie within a projected distance of 1au (Defrère et al. 2015), less than the 3au predicted by modelling of the infrared spectrum (Lisse et al. 2011), with one possible resolution being that the warm dust component is clumpy. The disc-to-star flux ratio at  $12\mu\text{m}$  is 1.2, roughly two times higher than the detectable limit. Thus, assuming a Solar mass star, the curved lines in the left panel of Figure 1 show the level of astrometric signal that would result if 50% of the warm component were concentrated in a single clump near 1au (though a factor two overestimated, as  $\eta$  Corvi is 18pc distant). The astrometric signal would be a few micro-arcseconds for an optical mission, and around 10 mas for mid-IR observations. GRAVITY astrometric precision is on the order of a few  $\mu\text{as}$  and could detect such a star's displacement (Lacour et al. 2014). In the mid-IR, the astrometric capabilities of IRAC/Spitzer of  $\sim 20\text{mas}$  could be used to probe these azimuthal structures at longer wavelengths (Esplin & Luhman 2016). Thus, high precision astrometry provides a possible way to probe the azimuthal structure of warm dust.

The detection limits that were used on Fig. 2 were photometric but for specific systems, it is possible to go deeper. Indeed, it might be possible to rule out a dust spot scenario using nulling interferometry (LBTI), which can go a few orders of magnitude deeper (Defrère et al. 2016). However, LBTI requires bright stars, so this option would only be available for the nearest stars, which is the case of most interest as this is where astrometric measurements are most sensitive.

Gaia is going to detect at least 20,000 Jupiter-mass planets or larger (Perryman et al. 2014). The astrometric effect of such planets is rather large ( $> 100\mu\text{as}$  according to Eq. 3) and for most stellar types it would mean that if dust was mimicking these planets, it would be detectable. It is clearly shown on Fig. 2 where a Jupiter-like planet with  $\Delta\alpha = 100\mu\text{as}$  lies above the sensitivity line when observed in the optical. We note that there are more bands than WISE  $12\mu\text{m}$  and they could also be used. Hence, a lack of an IR-excess rules out the possibility that an astrometric detection is dust but an IR-excess does not mean the planet is not real, since the dust could be axisymmetric.

Another source of perturbation is the transit of a planet. Indeed, from the ingress to the egress of the transit, the photo-centre of the stellar surface is displaced by an angle  $2\alpha_*(R_p/R_*)^3$ , where  $\alpha_*$  is the angular size of the host star and  $R_p$  ( $R_*$ ) is the planet (star) radius (Schneider 1999). It leads to an astrometric effect of  $2\mu\text{as}$  for a Jupiter transiting a K dwarf at 50 pc. But it cannot mimic a dynamical perturbation by a planet since its duration is only that of the transit, i.e. a few hours. Nevertheless, similar transits can be useful to investigate the inner structure of discs (Rodriguez et al. 2015). Indeed, if the disc is seen nearly edge on, its inhomogeneities with an orbital period of a few years leading to an astrometric effect could be investigated further by their transits. The depth and duration of the transit give the optical depth and size of the inhomogeneity, which can be used to model a pseudo-astrometric displacement of the photo-centre. That measurement would help to disentangle a planet-like astrometric effect from a pseudo-astrometric effect due to a disc inhomogeneity.

## 6. Conclusion

Here we have explored an artefact to be taken into account in any future astrometric detection of exoplanets. We find that dust clouds with cometary masses orbiting close to their host stars (within  $\sim 1$  arcsec) produce enough flux to mimic an Earth-like planet at 10pc. We have shown that one can expect a large diversity of situations to produce these inhomogeneities, so that, in future observations each case shall require a specific analysis. Astrometric observations around protoplanetary discs can also be affected by dust inhomogeneities as we have shown in section 3.2. We suggest that the astrometric signal observed around VB10 (potentially the first astrometric detection of a planet), which does not present any radial velocity might be explained by a massive dust cloud orbiting VB10 rather than a Jupiter-like planet. Our method can be used for the coming astrometric detection of thousands of planets with Gaia to rule out potential dust clumps. In any case, the most secure test to confirm a planet detection with astrometry shall be to check for the achromaticity of the astrometric measurement, and radial velocity measurements whenever possible. However, finding systems that are not achromatic would be interesting as it would reveal the detection of a certain amount of dust within the inner parts of planetary systems. This provides a new technique to probe the unresolved part of planetary systems and check for asymmetries due to dust clouds, exozodis or other inhomogeneities presented in this paper.

*Acknowledgements.* QK acknowledges support from the European Union through ERC grant number 279973D. GMK is supported by the Royal Society as a Royal Society University Research Fellow. Souami thanks the "Action Féderatrice Exoplanètes" of the Paris Observatory for financial support. QK wishes to thank J.-C. Augereau for fruitful discussions about GRaTeR. JS wishes to thank Didier Queloz for an initial discussion.

## References

- Absil, O., Debrère, D., Coudé du Foresto, V., et al. 2013, A&A, 555, A104
- Anglada-Escudé, G., Shkolnik, E. L., Weinberger, A. J., et al. 2010, ApJ, 711, L24
- Ansdell, M., Gaidos, E., Rappaport, S. A., et al. 2016, ApJ, 816, 69
- Augereau, J. C., Lagrange, A. M., Mouillet, D., Papaloizou, J. C. B., & Grorod, P. A. 1999, A&A, 348, 557
- Augereau, J. C., & Papaloizou, J. C. B. 2004, A&A, 414, 1153
- Bean, J. L., Seifahrt, A., Hartman, H., et al. 2010, ApJ, 711, L19
- Beust, H., Lagrange, A.-M., Crawford, I. A., et al. 1998, A&A, 338, 1015
- Boccaletti, A., Thalmann, C., Lagrange, A.-M., et al. 2015, Nature, 526, 230
- Braga-Ribas, F., Sicardy, B., Ortiz, J. L., et al. 2014, Nature, 508, 72
- de Bruijne, J. H. J. 2012, Ap&SS, 341, 31
- Debrère, D., Hinz, P. M., Skemer, A. J., et al. 2015, ApJ, 799, 42
- Debrère, D., Hinz, P. M., Mennesson, B., et al. 2016, arXiv:1601.06866
- Ertel, S., Augereau, J.-C., Absil, O., et al. 2015, The Messenger, 159, 24
- Esplin, T. L., & Luhman, K. L. 2016, AJ, 151, 9
- Faure, J., Fromang, S., Latter, H., & Meheut, H. 2015, A&A, 573, A132
- Flaherty, K. M., Muzerolle, J., Wolk, S. J., et al. 2014, ApJ, 793, 2
- Fomalont, E., & Reid, M. 2004, New A Rev., 48, 1473
- Fu, W., Li, H., Lubow, S., & Li, S. 2014, ApJ, 788, L41
- Garufi, A., Quanz, S. P., Avenhaus, H., et al. 2013, A&A, 560, A105
- Kennedy, G. M., & Wyatt, M. C. 2011, MNRAS, 412, 2137
- Kiefer, F., Lecavelier des Etangs, A., Augereau, J.-C., et al. 2014, A&A, 561, L10
- Kral, Q., Thébault, P., & Charnoz, S. 2013, A&A, 558, A121
- Kral, Q., Thébault, P., Augereau, J.-C., Boccaletti, A., & Charnoz, S. 2015, A&A, 573, A39
- Lacour, S., Eisenhauer, F., Gillessen, S., et al. 2014, Proc. SPIE, 9146, 91462E
- Lagrange, A.-M., Meunier, N., Desort, M., & Malbet, F. 2011, A&A, 528, L9
- Lebreton, J., van Lieshout, J.-C., Augereau, J.-Ch., Absil, O. et al. 2013, A&A, 555, A146
- Lesur, G., & Papaloizou, J. C. B. 2010, A&A, 513, A60
- Lesur, G., Hennebelle, P., & Fromang, S. 2015, A&A, 582, L9
- Lisse, C. M., Chen, C. H., Wyatt, M. C., et al. 2011, Lunar and Planetary Science Conference, 42, 2438
- Lovell, R. V. E., Li, H., Colgate, S. A., & Nelson, A. F. 1999, ApJ, 513, 805
- Lyra, W., & Lin, M.-K. 2013, ApJ, 775, 17
- Malbet, F., Léger, A., Shao, M., et al. 2012, Experimental Astronomy, 34, 385
- Meru, F. 2015, MNRAS, 454, 2529
- Montesinos, M., Perez, S., Casassus, S., et al. 2016, arXiv:1601.07912
- Muterspaugh, M. W., Lane, B. F., Kulkarni, S. R., et al. 2010, AJ, 140, 1657
- Perryman, M., Hartman, J., Bakos, G. Á., & Lindgren, L. 2014, ApJ, 797, 14
- Pravdo, S. H., & Shaklan, S. B. 2009, ApJ, 700, 623
- Rodriguez, J., Pepper, J., & Stassun, K. 2015, in Young Stars & Planets Near the Sun. arXiv:1509.04351
- Sahlmann, J., Burgasser, A. J., Martín, E. L., et al. 2015, A&A, 579, A61
- Sanders, G. H. 2013, Journal of Astrophysics and Astronomy, 34, 81
- Schneider, J., 1999, Extrasolar Planets Transits. in From extrasolar planets to cosmology: the VLT opening symposium. Springer 1999, p. 499
- Schneider, J. 2011. Astrophysical artefact in the astrometric detection of exoplanets. Oral Presentation at the Gaia Colloquium Pas de Deux. luth7.obspm.fr/Astrom-discs.pdf
- Shannon, A., Mustill, A. J., & Wyatt, M. 2015, MNRAS, 448, 684
- Smith, R., Wyatt, M. C., & Haniff, C. A. 2009, A&A, 503, 265
- Tanaka, H., Takeuchi, T., & Ward, W. R. 2002, ApJ, 565, 1257
- van der Marel, N., van Dishoeck, E. F., Bruderer, S., et al. 2013, Science, 340, 1199.
- Wyatt, M. C., Dermott, S. F., Grogan, K., & Jayaraman, S. 1999, Astrophysics with Infrared Surveys: A Prelude to SIRTf, 177, 374
- Wyatt, M. C., & Dent, W. R. F. 2002, MNRAS, 334, 589
- Wyatt, M. C., Greaves, J. S., Dent, W. R. F., & Coulson, I. M. 2005, ApJ, 620, 492
- Zeegers, S. T., Kenworthy, M. A., & Kalas, P. 2014, MNRAS, 439, 488